Structural Engineering and Mechanics, Vol. 6, No. 2 (1998) 229-243
DOI: http://dx.doi.org/10.12989/sem.1998.6.2.229

Vibration of T-type Timoshenko frames subjected to moving loads

Rong-Tyai Wang†

Department of Engineering Science, National Cheng Kung, University, Tainan, Taiwan, R.O.C.

Jin-Sheng Lin‡

Housing and Urban Development Bureau, Taiwan, R.O.C.

Abstract. In this study, a theoretical method to analyze the vibration of a T-type Timoshenko frame is proposed. The effects of axial inertia, rotatory inertia and shear deformation of each branch are considered. The orthogonality of any two distinct sets of mode shape functions is also demonstrated. Vibration of the frame due to moving loads is studied by the method and the response characteristics of the frame are investigated. Furthermore, the effect of column length on the response of the frame is also studied.

Key words: Timoshenko frame; orthogonality; moving loads.

1. Introduction

The vibration of frames is normally studied with the Bernoulli-Euler beam theory (Rubinstein and Hurty 1961, Levien and Hartz 1963). The theory leads to more erroneous results for beams with a large ratio of radius of gyration of cross section to length (Clough 1955). Moreover, the velocity of bending wave predicated by the theory is unreasonable within the high frequency range (Kolsky 1963). The error due to the theory can be fortunately corrected by including the effect of rotatory inertia and shear deformation of beam (Timoshenko 1921). Numerous studies based on the Timoshenko beam theory have been reported in previous literature (Herrmann 1955, Huang 1961, Sheng, *et al.* 1994). The Timoshenko beam theory has also been extended to study the vibration of frames (Cheng 1970, Warburton and Henshell 1969, Wang and Kinsman 1971). A frame is not in equilibrium without including the axial inertia effect of every branch of the frame. In studying the vibration of frame structures, the effects of axial inertia, rotatory inertia and shear deformation of every branch must be simultaneously considered (Wang and Jeng 1996).

T-type frames subjected to moving loads are widely encountered in elevated guideways. The finite element method has been adopted to study the problem of a T-type frame subjected to a moving concentrated load (Wang and Jeng 1996). Results indicate that the first modal frequency of a Timoshenko frame is less than that of a Bernoulli-Euler frame. Moreover, the maximum deflection of the Bernoulli-Euler frame is less than that of the Timoshenko frame. Furthermore, the

† Associate Professor
‡ Technician

cost of computational time causes the finite element method to be an inefficient tool for studying the problems of moving loads on frames. Consequently, a more efficient method of analyzing the vibration of Timoshenko frames must be investigated.

In this study, transfer matrix and analytical method are combined to calculate the modal frequencies and their corresponding mode shape functions of a T-type frame. The orthogonality of any two distinct sets of the mode shape functions has also been investigated to guarantee the appropriateness of the modal analysis method. A concentrated load and a uniformly distributed load moving on a T-type frame at a constant velocity are taken as two examples. Numerical results obtained by the method are, therefore, presented herein the paper to demonstrate the responses characteristics of the T-type frame due to moving loads. Furthermore, the effect of column length on the responses of the frame is also studied.

2. Equations of motion

Fig. 1 shows a T-type Timoshenko frame subjected to a uniformly distributed load $f(x, t)$. The frame structure contains three homogeneous and isotropic branches with Young's modulus E, shear modulus G, Poisson's ratio μ, density ρ and shear coefficient κ. This figure also presents the series number of each branch. The ith branch has length L_i, cross-sectional area A_i, and moment of area I_i. Furthermore, the axial force, transverse shear force and bending moment of the ith branch are denoted, respectively, as n_i, q_i, and m_i which are

$$n_i = EA_i \frac{\partial u_i}{\partial x_i}, \quad q_i = \kappa GA_i \left(\frac{\partial w_i}{\partial x_i} - \psi_i \right), \quad m_i = -EI_i \frac{\partial \psi_i}{\partial x_i} \tag{1}$$

where x_i is the axial coordinate, u_i is the longitudinal displacement, w_i is the transverse displacement and ψ_i is the bending slope. The applied forces and displacements at both ends of the ith branch (see Fig. 2) are denoted as

$$\{u \ w \ \psi\}_{ia}(t) = \{u \ w \ \psi\}_i(0, t), \ \{n \ q \ m\}_{ia}(t) = \{-n \ -q \ m\}_i(0, t) \tag{2a}$$

$$\{u \ w \ \psi\}_{ib}(t) = \{u \ w \ \psi\}_i(L_i, t), \ \{n \ q \ m\}_{ib}(t) = \{n \ q \ -m\}_i(L_i, t) \tag{2b}$$

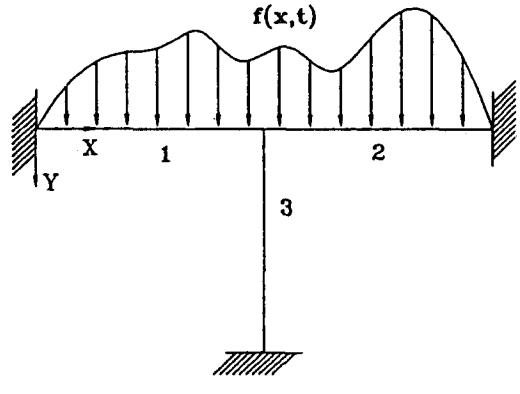

Fig. 1 A uniformly distributed load $f(x, t)$ on a T-type frame.

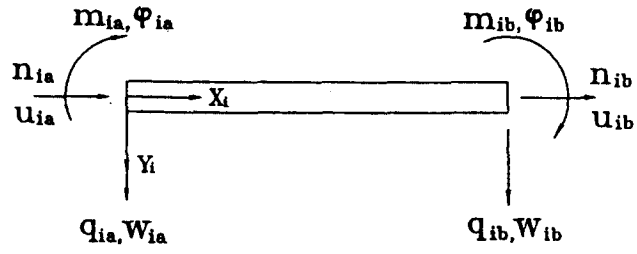

Fig. 2 Applied end forces and displacements for the *i*th branch.

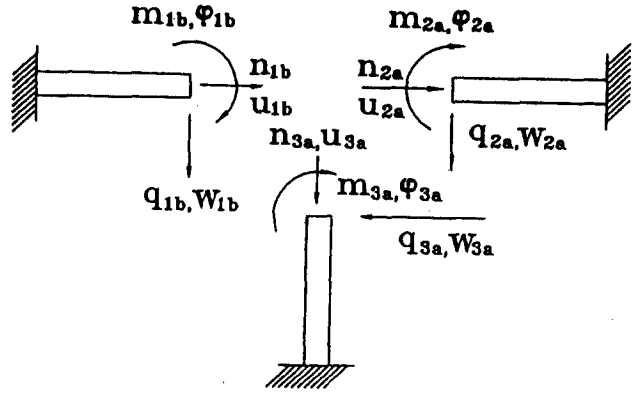

Fig. 3 Applied forces and displacements at the conjunction of three branches.

to correspond with the sign convention of displacements and forces presented by Warburton (1976). The equations of motion of two horizontal branches are as follows:

$$\frac{\partial n_i}{\partial x_i} = \rho A_i \frac{\partial^2 u_i}{\partial t^2} \tag{2a}$$

$$\frac{\partial q_i}{\partial x_i} + f(x_i, t) = \rho A_i \frac{\partial^2 w_i}{\partial t^2} \tag{2b}$$

$$q_i - \frac{\partial m_i}{\partial x_i} = \rho I_i \frac{\partial^2 \psi_i}{\partial t^2}, \quad i = 1, 2 \tag{2c}$$

Furthermore, the equations of motion of the vertical branch are

$$\frac{\partial n_3}{\partial x_3} = \rho A_3 \frac{\partial^2 u_3}{\partial t^2} \tag{3a}$$

$$\frac{\partial q_3}{\partial x_3} = \rho A_3 \frac{\partial^2 w_3}{\partial t^2} \tag{3b}$$

$$q_3 - \frac{\partial m_3}{\partial x_3} = \rho I_3 \frac{\partial^2 \psi_3}{\partial t^2} \tag{3c}$$

The boundary conditions of the fixed ends of the frame are

$$u_{1a}(t) = u_{2b}(t) = u_{3b}(t) = 0, \quad w_{1a}(t) = w_{2b}(t) = w_{3b}(t) = 0,$$
$$\psi_{1a}(t) = \psi_{2b}(t) = \psi_{3b}(t) = 0 \tag{4a}$$

Moreover, the forces balance and displacements continuity at the junction of three branches (see Fig. 3) are

$$\psi_{1b}(t)=\psi_{2a}(t)=\psi_{3a}(t),\ u_{1b}(t)=u_{2a}(t)=-w_{3a}(t),$$
$$w_{1b}(t)=w_{2a}(t)=u_{3a}(t) \tag{4b}$$
$$m_{1b}(t)+m_{2a}(t)+m_{3a}(t)=0,\ q_{1b}(t)+q_{2a}(t)+n_{3a}(t)=0,$$
$$n_{1b}(t)+n_{2a}(t)-q_{3a}(t)=0 \tag{4c}$$

Eqs. (1)-(4c) constitute the equations of motion of the T-type frame.

3. Modal frequencies

To calculate the modal frequencies of the frame, the displacement components, bending slope, axial force, transverse shear force and bending moment of the ith branch are expressed as

$$\{u\ w\ \psi\}_i(x_i,t)=\{U\ W\ \Psi\}_i(x_i)\sin(\omega t) \tag{5a}$$
$$\{n\ q\ m\}_i(x_i,t)=\{N\ Q\ M\}_i(x_i)\sin(\omega t) \tag{5b}$$

in which ω is the circular frequency. The corresponding longitudinal displacement $U_i(x_i)$ and two axially nodal forces N_{ia} and N_{ib} are

$$U_i(x_i)=B_{1i}\cos(\lambda x_i)+B_{2i}\sin(\lambda x_i) \tag{6a}$$
$$N_{ia}=-EA_i\lambda B_{2i} \tag{6b}$$
$$N_{ib}=EA_i\lambda\{-B_{1i}\sin(\lambda L_i)+B_{2i}\cos(\lambda L_i)\} \tag{6c}$$

where, B_{1i} and B_{2i} are two constants and $\lambda=(\rho/E)^{1/2}\omega$. The radius of gyration of the cross section of beams is denoted as η_i. The transverse displacement, bending slope, bending moment and shear force of a Timoshenko beam can be found in Huang's paper (1961). In this study, the transverse displacement $W_i(x_i)$, bending slope $\Psi_i(x_i)$, two bending moments M_{ia} and M_{ib} and transversely shear forces Q_{ia} and Q_{ib} at the nodes are given by

case 1: for $\lambda^2<\dfrac{\kappa}{2(1+\mu)\eta_i^2}$

$$W_i(x_i)=B_{3i}\cosh(p_{1i}x_i)+B_{4i}\sinh(p_{1i}x_i)+B_{5i}\cos(p_{2i}x_i)+B_{6i}\sin(p_{2i}x_i) \tag{7a}$$
$$\Psi_i(x_i)=\beta_1(p_{1i})[B_{4i}\cosh(p_{1i}x_i)+B_{3i}\sinh(p_{1i}x_i)]+\beta_2(p_{2i})[B_{5i}\sin(p_{2i}x_i)-B_{6i}\cos(p_{2i}x_i)] \tag{7b}$$
$$Q_{ia}=-\gamma(p_{1i})B_{4i}+\gamma(p_{2i})B_{6i} \tag{7c}$$
$$Q_{ib}+\gamma(p_{1i})[B_{3i}\sinh(p_{1i}L_i)+B_{4i}\cosh(p_{1i}L_i)]+\gamma(p_{2i})[B_{5i}\sin(p_{2i}L_i)-B_{6i}\cos(p_{2i}L_i)] \tag{7d}$$
$$M_{ia}=-\alpha_1(p_{1i})B_{3i}-\alpha_2(p_{2i})B_{5i} \tag{7e}$$
$$M_{ib}=\alpha_1(p_{1i})[B_{3i}\cosh(p_{1i}L_i)+B_{4i}\sinh(p_{1i}L_i)]+\alpha_2(p_{2i})[B_{5i}\cos(p_{2i}L_i)+B_{6i}\sin(p_{2i}L_i)] \tag{7f}$$

where the parameters p_{1i} and p_{2i}, the functions $\beta_1(\ )$, $\beta_2(\ )$, $\alpha_1(\ )$, $\alpha_2(\ )$ and $\gamma(\ )$ are

$$p_{1i}^2=-\frac{\lambda^2}{2}\left[1+\frac{2(1+\mu)}{\kappa}\right]+\left\{\frac{\lambda^4}{4}\left[1+\frac{2(1+\mu)}{\kappa}\right]^2+\left[\frac{\lambda^2}{\eta_i^2}-\frac{2(1+\mu)\lambda^4}{\kappa}\right]\right\}^{1/2}>0,$$

$$p_{2i}^2 = -\frac{\lambda^2}{2}\left[1+\frac{2(1+\mu)}{\kappa}\right]+\left\{\frac{\lambda^4}{4}\left[1+\frac{2(1+\mu)}{\kappa}\right]^2+\left[\frac{\lambda^2}{\eta_i^2}-\frac{2(1+\mu)\lambda^4}{\kappa}\right]\right\}^{1/2} > 0,$$

$$\beta_1(p)=\frac{1}{p}\left[p^2+\frac{2(1+\mu)\lambda^2}{\kappa}\right],\ \beta_2(p)=\frac{1}{p}\left[-p^2+\frac{2(1+\mu)\lambda^2}{\kappa}\right],$$

$$\alpha_1(p)=EI_i\left[p^2+\frac{2(1+\mu)\lambda^2}{\kappa}\right],\ \alpha_2(p)=EI_i\left[-p^2+\frac{2(1+\mu)\lambda^2}{\kappa}\right]$$

$$\gamma(p)=-\frac{2(1+\mu)\lambda^2 GA_i}{p}$$

case 2: for $\lambda^2 > \dfrac{\kappa}{2(1+\mu)\eta_i^2}$

$$W_i(x_i)=B_{1i}\cos(p_{1i}x_i)+B_{2i}\sin(p_{1i}x_i)+B_{3i}\cos(p_{2i}x_i)+B_{4i}\sin(p_{2i}x_i) \quad (8a)$$

$$\Psi_i(x_i)=\beta_2(p_{1i})[B_{3i}\sin(p_{1i}x_i)-B_{4i}\cos(p_{1i}x_i)]+\beta_2(p_{2i})[B_{5i}\sin(p_{2i}x_i)-B_{6i}\cos(p_{2i}x_i)] \quad (8b)$$

$$Q_{ia}=\gamma(p_{1i})B_{4i}+\gamma(p_{2i})B_{6i} \quad (8c)$$

$$Q_{ib}=\gamma(p_{1i})[B_{3i}\sin(p_{1i}L_i)-B_{4i}\cos(p_{1i}L_i)]+\gamma(p_{2i})[B_{5i}\sin(p_{2i}L_i)-B_{6i}\cos(p_{2i}L_i)] \quad (8d)$$

$$M_{ia}=-\alpha_2(p_{1i})B_{3i}-\alpha_2(p_{2i})B_{5i} \quad (8e)$$

$$M_{ib}=+\alpha_2(p_{1i})[B_{3i}\cos(p_{1i}L_i)+B_{4i}\sin(p_{1i}L_i)]+\alpha_2(p_{2i})[B_{5i}\cos(p_{2i}L_i)+B_{6i}\sin(p_{2i}L_i)] \quad (8f)$$

where the parameters p_{1i} and p_{2i}, the functions $\beta_2(\ )$, $\alpha_2(\ )$ and $\gamma(\ )$ are

$$p_{1i}^2=\frac{\lambda^2}{2}[1+\frac{2(1+\mu)}{\kappa}]-\{\frac{\lambda^4}{4}[1+\frac{2(1+\mu)}{\kappa}]^2+[\frac{\lambda^2}{\eta_i^2}-\frac{2(1+\mu)\lambda^4}{\kappa}]\}^{1/2} > 0,$$

$$p_{2i}^2=\frac{\lambda^2}{2}[1+\frac{2(1+\mu)}{\kappa}]+\{\frac{\lambda^4}{4}[1+\frac{2(1+\mu)}{\kappa}]^2+[\frac{\lambda^2}{\eta_i^2}-\frac{2(1+\mu)\lambda^4}{\kappa}]\}^{1/2} > 0,$$

$$\beta_2(p)=\frac{1}{p}[-p^2+\frac{2(1+\mu)\lambda^2}{\kappa}],\quad \alpha_2(p)=EI_i[-p^2+\frac{2(1+\mu)\lambda^2}{\kappa}]$$

$$\gamma(p)=-\frac{2(1+\mu)\lambda^2 GA_i}{p}$$

All B_{ji} are constant for i=1~3 and j=3~6.

Eqs. (6a)-(6c) and (7a)-(7f) or Eqs. (6a)-(6c) and (8a)-(8f) may be symbolically arranged into the vector forms as

$$\{D_l\ \ F_l\}_i^T=[R]_i\,\vec{B}_i,\quad i=1\sim3 \quad (9a)$$

$$\{D_r\ \ F_r\}_i^T=[K]_i\,\vec{B}_i,\quad i=1\sim3 \quad (9b)$$

where,

$$\vec{B}_i=\{B_1\ B_2\ B_3\ B_4\ B_5\ B_6\}_i^T,\qquad i=1\sim3$$

$$\{D_r\}_i = \{U_{ib} \;\; W_{ib} \;\; \Psi_{ib}\}^T, \quad \{D_l\}_i = \{U_{ia} \;\; W_{ia} \;\; \Psi_{ia}\}^T$$
$$\{F_r\}_i = \{N_{ib} \;\; Q_{ib} \;\; M_{ib}\}^T, \quad \{F_l\}_i = \{N_{ia} \;\; Q_{ia} \;\; M_{ia}\}^T, \qquad i = 1, 2$$
$$\{D_r\}_3 = \{-W_{3b} \;\; U_{3b} \;\; \Psi_{3b}\}^T; \quad \{D_l\}_3 = \{-W_{3a} \;\; U_{3a} \;\; \Psi_{3a}\}^T$$
$$\{F_r\}_3 = \{-Q_{3b} \;\; N_{3b} \;\; M_{3b}\}^T; \quad \{F_l\}_3 = \{-Q_{3a} \;\; N_{3a} \;\; M_{3a}\}^T$$

By solving the constant vector $\vec{B}_i$ in terms of $\{D_l\}_i$ and $\{F_l\}_i$ from Eq. (9a), then substituting the constant vector into Eq. (9b) and arranging the results to the desired form yields

$$\begin{Bmatrix} D_r \\ F_r \end{Bmatrix}_i = \begin{bmatrix} Z_{11} & Z_{12} \\ Z_{21} & Z_{22} \end{bmatrix}_i \begin{Bmatrix} D_l \\ F_l \end{Bmatrix}_i, \qquad i = 1 \sim 3 \tag{10}$$

Employing the boundary conditions of fixed bottom of the third branch into Eq. (10) yields the force-displacement relation at the top of the branch in the form

$$\{F_l\}_3 = -[Z^*]_3 \{D_l\}_3 \tag{11}$$

where, $[Z^*]_3=[Z_{12}]_3^{-1}[Z_{11}]_3$. The conditions of displacements continuity and forces balance at the junction of these branches are

$$\{D_r\}_1 = \{D_l\}_3 = \{D_l\}_2 \tag{12a}$$
$$\{F_l\}_3 + \{F_r\}_1 + \{F_l\}_2 = \{0 \;\; 0 \;\; 0\}^T \tag{12b}$$

Combining Eqs. (11)-(12b) yields

$$\begin{Bmatrix} D_l \\ F_l \end{Bmatrix}_2 = \begin{bmatrix} I_{3\times 3} & O \\ Z_3^* & -I_{3\times 3} \end{bmatrix} \begin{Bmatrix} D_r \\ F_r \end{Bmatrix}_1 \tag{13}$$

where $I_{3\times 3}$ is an identity matrix of order 3 and O is a zero matrix. Substituting Eq. (13) into Eq. (10) yields

$$\begin{Bmatrix} D_r \\ F_r \end{Bmatrix}_2 = \begin{bmatrix} P_{11} & P_{12} \\ P_{21} & P_{22} \end{bmatrix} \begin{Bmatrix} D_l \\ F_l \end{Bmatrix}_1 \tag{14}$$

in which

$$\begin{bmatrix} P_{11} & P_{21} \\ P_{21} & P_{22} \end{bmatrix} = \begin{bmatrix} Z_{11} & Z_{12} \\ Z_{21} & Z_{22} \end{bmatrix}_2 \begin{bmatrix} I_{3\times 3} & O \\ Z_3^* & -I_{3\times 3} \end{bmatrix} \begin{bmatrix} Z_{11} & Z_{12} \\ Z_{21} & Z_{22} \end{bmatrix}_1$$

The boundary conditions of

$$\{D_l\}_1 = \{0 \;\; 0 \;\; 0\}^T, \quad \{D_r\}_2 = \{0 \;\; 0 \;\; 0\}^T \tag{16}$$

imply that the jth modal frequency ω_j and the corresponding eigenvector $\{F_l\}_{1,j}$ satisfy

$$[P_{12}]\{F_l\}_1 = \{0\ 0\ 0\}^T \tag{17}$$

$\{D_l\}_{1,j}$ is always a zero vector. Substituting $\{F_l\}_{1,j}$ and $\{D_l\}_{1,j}$ into Eq. (10) yields $\{F_r\}_{1,j}$ and $\{D_r\}_{1,j}$. $\{F_l\}_{2,j}$ and $\{D_l\}_{2,j}$ can then be obtained by solving Eq. (13). Moreover, $\{F_l\}_{3,j}$ and $\{D_l\}_{3,j}$ are obtained from Eqs. (12a) and (12b). The corresponding constant vectors $\vec{B}_{i,j}$ is then obtained by solving Eq. (9a). Substituting the vectors $\vec{B}_{i,j}$ into Eqs. (6a)-(6c) and Eqs. (7a)-(7f) or (8a)-(8f) yields the jth mode shape functions of longitudinal displacement $U_{i,j}(x_i)$, transverse deflection $W_{i,j}(x_i)$, rotatory angle $\Psi_{i,j}(x_i)$, axial force $N_{i,j}(x_i)$, shear force $Q_{i,j}(x_i)$ and bending moment $M_{i,j}(x_i)$ of the ith branch, where i=1~3.

4. Orthogonality of mode shape functions

The set of the jth mode shape functions $\{U_{i,j}\ W_{i,j}\ \Psi_{i,j}\}(x_i)$ of the ith branch satisfies the following equations,

$$\rho A_i \omega_j^2 U_{i,j} = -\frac{dN_{i,j}}{dx_i} \tag{18a}$$

$$\rho A_i \omega_j^2 W_{i,j} = -\frac{dQ_{i,j}}{dx_i} \tag{18b}$$

$$\rho I_i \omega_j^2 \Psi_{i,j} = -Q_{i,j} + \frac{dM_{i,j}}{dx_i} \qquad i = 1, 2, 3 \tag{18c}$$

By omitting the description of the procedures of derivation, the following equations are obtained

$$\rho A_i(\omega_j^2 - \omega_k^2)\int_0^{L_i} U_{i,j} U_{i,k}\, dx_i = N_{ib,k} U_{ib,j} + N_{ia,k} U_{ia,j} - N_{ib,j} U_{ib,k} - N_{ia,j} U_{ia,k} \tag{19a}$$

$$\begin{aligned}\rho A_i(\omega_j^2 - \omega_k^2)\int_0^{L_i} W_{i,j} W_{i,k}\, dx_i &= \int_0^{L_i}\left(-Q_{i,k}\frac{dW_{i,j}}{dx_i} + Q_{i,j}\frac{dW_{i,k}}{dx_i}\right)dx_i \\ &+ Q_{ib,k} W_{ib,j} + Q_{ia,k} W_{ia,j} - Q_{ib,j} W_{ib,k} - Q_{ia,j} W_{ia,k}\end{aligned} \tag{19b}$$

$$\begin{aligned}\rho I_i(\omega_j^2 - \omega_k^2)\int_0^{L_i} \Psi_{i,j} \Psi_{i,k}\, dx_i &= \int_0^{L_i}(Q_{i,k}\Psi_{i,j} - Q_{i,j}\Psi_{i,k})\, dx_i \\ &+ M_{ib,k}\Psi_{ib,j} + M_{ia,k}\Psi_{ia,j} - M_{ib,j}\Psi_{ib,k} - M_{ia,j}\Psi_{ia,k}\end{aligned} \tag{19c}$$

Performing the summation of Eqs. (19a), (19b) and (19c) for i=1-3 then adopting the conditions of Eqs. (12a) and (12b) into the result yields the orthogonality of any two distinct sets of the mode shape functions

$$(\omega_j^2 - \omega_k^2)\sum_{i=1}^{3}\int_0^{L_i}\left(\rho A U_{i,j} U_{i,k} + \rho A W_{i,j} W_{i,k} + \rho I \Psi_{i,j} \Psi_{i,k}\right)dx_i = 0, \qquad j \neq k \tag{20a}$$

which also implies

$$\sum_{i=1}^{3}\int_0^{L_i}\left[U_{i,k}\frac{dN_{i,j}}{dx_i} + W_{i,k}\frac{dQ_{i,j}}{dx_i} + \Psi_{i,k}\left(Q_{i,j} - \frac{dM_{i,j}}{dx_i}\right)\right]dx_i = 0 \tag{20b}$$

5. Forced vibration

While studying the forced vibration, the responses of each branch can be expanded into the generalized Fourier series forms of

$$\{u, w, \psi\}_i (x_i, t) = \sum_{k=1} c_k (t) \{U, W, \Psi\}_{i,k} (x_i) \qquad i = 1, 2, 3 \tag{21a}$$

$$\{n, q, m\}_i (x_i, t) = \sum_{k=1} c_k (t) \{N, Q, M\}_{i,k} (x_i) \qquad i = 1, 2, 3 \tag{21b}$$

in which $c_k(t)$ is the kth modal amplitude. Substituting Eqs. (21a) and (21b) into Eq. (3a) or Eq. (4a), then multiplying by $U_{i,j}(x_i)$ and integrating the result from x_i=0 to x_i=L_i yields

$$\sum_{k=1} c_k \int_0^{L_i} U_{i,j} \frac{dN_{i,k}}{dx_i} dx_i = \sum_{k=1} \frac{d^2 c_k}{dt^2} \int_0^{L_i} \rho A_i U_{i,j} U_{i,k} dx_i , \qquad i = 1 \sim 3 \tag{22a}$$

Similarly, the following equations can be obtained

$$\sum_{k=1} c_k \int_0^{L_i} W_{i,j} \frac{dQ_{i,k}}{dx_i} dx_i + \int_0^{L_i} f(x_i, t) W_{i,k} dx_i = \sum_{k=1} \frac{d^2 c_k}{dt^2} \int_0^{L_i} \rho A_i W_{i,j} W_{i,k} dx_i , \qquad i = 1, 2 \tag{22b}$$

$$\sum_{k=1} c_k \int_0^{L_3} W_{3,j} \frac{dQ_{3,k}}{dx_3} dx_3 = \sum_{k=1} \frac{d^2 c_k}{dt^2} \int_0^{L_3} \rho A_3 W_{3,j} W_{3,k} dx_3 \tag{22c}$$

$$\sum_{k=1} c_k \int_0^{L_i} \Psi_{i,j} \left(Q_{i,k} - \frac{dM_{i,k}}{dx_i} \right) dx_i = \sum_{k=1} \frac{d^2 c_k}{dt^2} \int_0^{L_i} \rho I_i \Psi_{i,j} \Psi_{i,k} dx_i , \qquad i = 1 \sim 3 \tag{22d}$$

Summing the values of Eqs. (22a)-(22d) and employing the conditions of Eqs. (20a) and (20b) into the above result yields

$$\frac{d^2 c_j}{dt^2} + \omega_j^2 c_j = g_j (t) \tag{23}$$

where ω_j is the jth modal frequency and the corresponding modal excitation is $g_i(t)$ is

$$g_j (t) = \sum_{i=1}^{2} \int_0^L f(x_i, t) W_{i,j} dx_i / s_j$$

in which s_j is the jth modal mass

$$s_j = \sum_{i=1}^{3} \int_0^{L_i} \left[\rho A_i (U_{i,j}^2 + W_{i,j}^2) + \rho I_i \Psi_{i,j}^2 \right] dx_i$$

6. Moving loads

In this section, we consider two types of moving loads, viz. concentrated load and uniformly distributed load.

6.1. Moving concentrated load

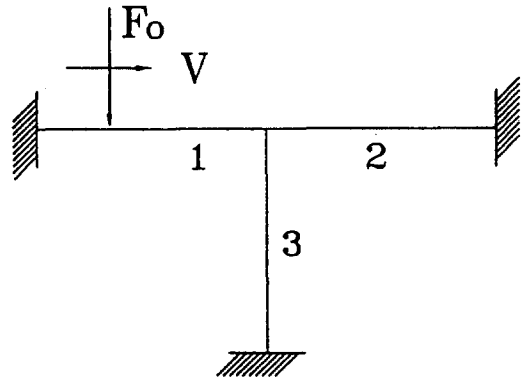

Fig. 4 A concentrated load moves on the T-type frame.

Fig. 4 depicts a concentrated load of magnitude F_0 moving at a constant velocity V on the frame. The form of the load is

$$f(x,t)=F_0\,\delta(x-Vt),\quad 0\le x\le L_1+L_2 \tag{24}$$

The histories of the jth modal excitation, amplitude and velocity of the frame, respectively, are

1) $0\le t\le T_1(=L_1/V)$

$$g_j(t)=F_0 W_{1,j}(Vt)/s_j \tag{25a}$$

$$c_j(t)=c_j(0)\cos(\omega_j t)+\dot{c}_j(0)\left(\frac{\sin(\omega_j t)}{\omega_j}\right)+\int_0^t\frac{\sin[\omega_j(t-\tau)]}{\omega_j}g_j(\tau)\,d\tau \tag{25b}$$

$$\dot{c}_j(t)=-\omega_j c_j(0)\sin(\omega_j t)+\dot{c}_j(0)\cos(\omega_j t)+\int_0^t\cos[\omega_j(t-\tau)]g_j(\tau)\,d\tau \tag{25c}$$

2) $T_1\le t\le T_2,\quad T_2=(L_1+L_2)/V$

$$g_j(t)=F_0 W_{2,j}(Vt)/s_j \tag{26a}$$

$$c_j(t)=c_j(T_1)\cos[\omega_j(t-T_1)]+\dot{c}_j(T_1)\left(\frac{\sin[\omega_j(t-T_1)]}{\omega_j}\right)+\int_{T_1}^t\frac{\sin[\omega_j(t-\tau)]}{\omega_j}g_j(\tau)\,d\tau \tag{26b}$$

$$\dot{c}_j(t)=-\omega_j c_j(T_1)\sin[\omega_j(t-T_1)]+\dot{c}_j(T_1)\cos[\omega_j(t-T_1)]+\int_{T_1}^t\cos[\omega_j(t-\tau)]\,g_j(\tau)\,d\tau \tag{26c}$$

3) $T_2<t$

$$g_j(t)=0 \tag{27a}$$

$$c_j(t)=c_j(T_2)\cos[\omega_j(t-T_2)]+\dot{c}_j(T_2)\left(\frac{\sin[\omega_j(t-T_2)]}{\omega_j}\right) \tag{27b}$$

$$\dot{c}_j(t)=-\omega_j\,c_j(T_2)\sin[\omega_j(t-T_2)]+\dot{c}_j(T_2)\cos[\omega_j(t-T_2)] \tag{27c}$$

6.2. Moving uniformly distributed load

Fig. 5 depicts the T-type frame subjected to a uniformly distributed load f_0 with a constant velocity V. The equation of the load is

$$f(\bar{x}, t) = f_0[H(x+d-Vt)-H(x-Vt)] \tag{28}$$

where H is the unit step function and the distributed length d is equal or less than both length of horizontal branches of the frame. The histories of the jth modal excitation, amplitude and velocity of the frame, respectively, are

1) $0 \le t \le t_1 (= d/V)$

$$g_j(t) = f_0 \int_0^{Vt} W_{1,j}(x_1)\, dx_1 / s_j \tag{29a}$$

$$c_j(t) = c_j(0)\cos(\omega_j t) + \dot{c}_j(0)\left(\frac{\sin(\omega_j t)}{\omega_j}\right) + \int_0^t \frac{\sin[\omega_j(t-\tau)]}{\omega_j} g_j(\tau)\, d\tau \tag{29b}$$

$$\dot{c}_j(t) = -\omega_j c_j(0)\sin(\omega_j t) + \dot{c}_j(0)\cos(\omega_j t) + \int_0^t \cos[\omega_j(t-\tau)]\, g_j(\tau)\, d\tau \tag{29c}$$

2) $t_1 \le t \le T_1$

$$g_j(t) = f_0 \int_{Vt-d}^{Vt} W_{1,j}(x_1)\, dx_1 / s_j \tag{30a}$$

$$c_j(t) = c_j(t_1)\cos[\omega_j(t-t_1)] + \dot{c}_j(t_1)\left(\frac{\sin[\omega_j(t-t_1)]}{\omega_j}\right) + \int_{t_1}^t \frac{\sin[\omega_j(t-\tau)]}{\omega_j} g_j(\tau)\, d\tau \tag{30b}$$

$$\dot{c}_j(t) = -\omega_j c_j(t_1)\sin[\omega_j(t-t_1)] + \dot{c}_j(t_1)\cos[\omega_j(t-t_1)] + \int_{t_1}^t \cos[\omega_j(t-\tau)]\, g_j(\tau)\, d\tau \tag{30c}$$

3) $T_1 \le t \le T_1 + t_1$

$$g_j(t) = f_0 \left(\int_{L_1}^{Vt} W_{2,j}(x_2)\, dx_2 + \int_{Vt-d}^{L_1} W_{1,j}(x_1)\, dx_1 \right) / s_j \tag{31a}$$

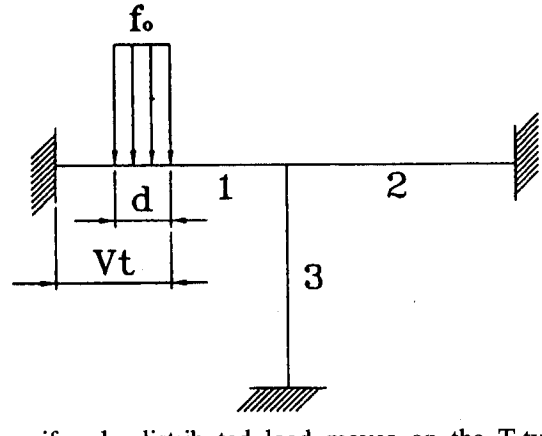

Fig. 5 A uniformly distributed load moves on the T-type frame.

$$c_j(t)=c_j(T_1)\cos[\omega_j\,(t-T_1)]+\dot{c}_j(T_1)\left(\frac{\sin[\omega_j(t-T_1)]}{\omega_j}\right)+\int_{T_1}^{t}\frac{\sin[\omega_j\,(t-\tau)]}{\omega_j}\,g_j\,(\tau)\,d\tau \quad (32b)$$

$$\dot{c}_j(t)=-\omega_j c_j(T_1)\sin[\omega_j(t-T_1)]+\dot{c}_j\,(T_1)\cos[\omega_j(t-T_1)]+\int_{T_1}^{t}\cos[\omega_j(t-\tau)]\,g_j(\tau)\,d\tau \quad (32c)$$

4) $T_1+t_1\le t\le T_2$

$$g_j(t)=f_0\int_{Vt-d}^{Vt}W_{2,j}\,(x_2)\,dx_2/s_j \quad (33a)$$

$$c_j(t)=c_j(T_1+t_1)\cos[\omega_j(t-T_1-t_1)]$$
$$+\dot{c}_j(T_1+t_1)\left(\frac{\sin(\omega_j(t-T_1-t_1)]}{\omega_j}\right)+\int_{T_1+t_1}^{t}\frac{\sin[\omega_j(t-\tau)]}{\omega_j}\,g_j(\tau)\,d\tau \quad (33b)$$

$$\dot{c}_j(t)=-\omega_j c_j\,(T_1+t_1)\sin[\omega_j(t-T_1-t_1)]+\dot{c}_j(T_1+t_1)\cos[\omega_j(t-T_1-t_1)]$$
$$+\int_{T_1+t_1}^{t}\cos[\omega_j(t-\tau)]\,g_j\,(\tau)\,d\tau \quad (33c)$$

5) $T_2\le t\le T_2+t_1$

$$g_j(t)=f_0\int_{Vt-d}^{VT_2}W_{2,j}\,(x_2)\,dx_2/s_j \quad (34a)$$

$$c_j(t)=c_j(T_2)\cos[\omega_j(t-T_2)]+\dot{c}_j\,(T_2)\left(\frac{\sin[\omega_j(t-T_2)]}{\omega_j}\right)+\int_{T_2}^{t}\frac{\sin[\omega_j(t-\tau)]}{\omega_j}\,g_j\,(\tau)\,d\tau \quad (34b)$$

$$\dot{c}_j(t)=-\omega_j c_j(T_2)\sin[\omega_j\,(t-T_2)]+\dot{c}_j(T_2)\cos[\omega_j(t-T_2)]+\int_{T_2}^{t}\cos[\omega_j(t-\tau)]\,g_j\,(\tau)\,d\tau \quad (34c)$$

6) $T_2+t_1\le t$

$$g_j\,(t)=0 \quad (35a)$$

$$c_j(t)=c_j(T_2+t_1)\cos[\omega_j\,(t-T_2-t_1)]+\dot{c}_j(T_2+t_1)\left(\frac{\sin[\omega_j\,(t-T_2-t_1)]}{\omega_j}\right) \quad (35b)$$

$$\dot{c}_j(t)=-\omega_j c_j(T_2+t_1)\sin[\omega_j(t-T_2-t_1)]+\dot{c}_j(T_2+t_1)\cos[\omega_j\,(t-T_2-t_1)] \quad (35c)$$

7. Examples

In this section, both horizontal branches are considered to have equal L length. Moreover, three branches of the frame have the same cross-sectional area A, moment of area I and the radius of gyration η of the cross-sectional area. To simplify the numerical computation in the paper, the non-dimensional variables are introduced as

$$\bar{u}_i=u_i/L,\quad \bar{w}_i=w_i/\eta,\quad \bar{\psi}_i=L\,\psi_i/\eta,\quad \bar{x}_i=x_i/L,\quad r_b=\eta/L,$$
$$\bar{n}_i=n_i/EA,\quad \bar{q}_i=q_iL^3/EI\,\eta,\quad \bar{m}_i=m_iL^2/EI\,\eta,\quad i=1,2$$

$$\bar{u}_3 = u_3/L_3,\quad \bar{w}_3 = w_3/\eta,\quad \bar{\psi}_3 = L_3\psi_3/\eta,\quad \bar{x}_i = x_i/L_i,\quad l_r = L_3/L,$$
$$\bar{n}_3 = n_3/EA,\quad \bar{q}_3 = q_3 L_3^3/EI\eta,\quad \bar{m}_3 = m_3 L_3^2/EI\eta,\quad \bar{V} = V(\rho/E)^{1/2}/r_b,$$
$$\bar{d} = d/L,\quad \bar{F}_0 = F_0 L^3/EI\eta,\quad \bar{f}_0 = f_0 L^4/EI\eta,\quad \bar{t} = (EI/\rho AL^4)^{1/2} t,\quad \varepsilon = E/\kappa G$$

where l_r is the length ratio of column to one horizontal beam. Moreover, the shear coefficient $\kappa = 2/3$ and Poisson's ratio $\mu = 1/3$ of each branch are considered in this section. Both values of $\bar{F}_0$ and $\bar{f}_0\,\bar{d}$ are assumed to be unity.

The following parameters are defined to illustrate the numerical results,

non-dimensional frequency, $\bar{\omega}(=100\omega(\rho/E)^{1/2}L)$;
maximum deflection during the motion of load, $\bar{W}_{max}$;
maximum moment during the motion of load, $\bar{M}_{max}$;
velocity ratio, $\alpha(=100V(\rho/E)^{1/2})$;
position of maximum deflection during the motion of load, $\bar{x}_W$;

Figs. 6(a)-6(c) display the lowest three modal frequencies and their corresponding mode shape of a T-type frame with r_b=0.03 and l_r=0.5. The first mode is the frame's bending mode. The result obtained by the modal analysis method converges rapidly. Therefore, the lowest sixteen modal frequencies and their corresponding mode shape functions of the frame are sufficient to be considered in the study of forced vibration of the structure. The initial conditions of the frame are set at zero. Furthermore, the velocity range $0 \le \alpha \le 16$ of loads is considered.

Fig. 7 displays the effects of two α values on the deflection histories of the middle point of the second branch of a frame with r_b=0.03 and l_r=0.5 induced by a concentrated moving load. This figure indicates that the maximum deflection at the point occurs during the load moves on the frame at a low speed. However, the maximum deflection occurs after the high speed load has left the frame.

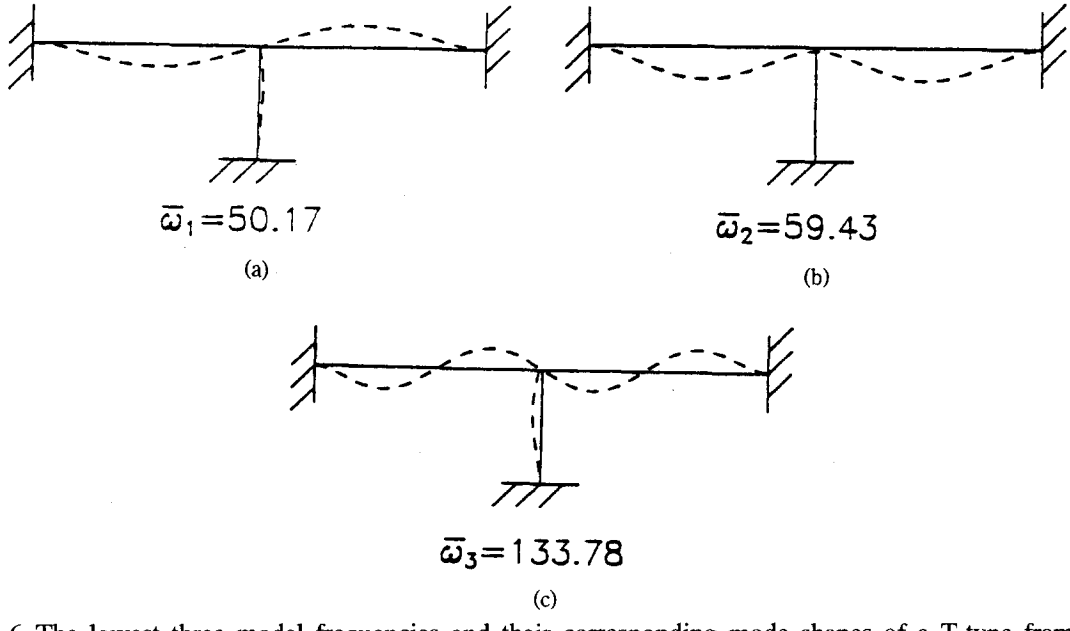

Fig. 6 The lowest three modal frequencies and their corresponding mode shapes of a T-type frame with r_b=0.03 and l_r=0.5: (A) the first mode, (b) the second mode and (c) the third mode.

Figs. 8(a) and 8(b) display the effects of distributed length of load on the $\overline{W}_{max}$-α and $\overline{M}_{max}$-α distributions, respectively, for a frame with r_b=0.03 and l_r=0.5. According to those figures, the more narrowly distributed length of load implies the larger the deflection and moment of the frame. Both figures reveal that there are two respective critical velocity α_W and α_M at which the maximum deflection and maximum moment become absolute maximum. Furthermore, the more narrow the load implies the more apparent both α_W and α_M of the frame are. Fig. 9 presents the $\bar{x}_W$-α distribution of the frame to a concentrated moving load, indicating that the maximum deflection always occurs at the middle point of one horizontal branch. The maximum moment of the horizontal branches always occurs at one fixed end of the frame.

Figs. 10(a) and 10(b) compare three l_r effects on the $\overline{W}_{max}$-α and $\overline{M}_{max}$-α distributions of a frame with r_b=0.03 to a concentrated moving load, respectively. Table 1 compares the effects of three different values of l_r on the fundamental three modal frequencies $\bar{\omega}$ of a T-type frame with

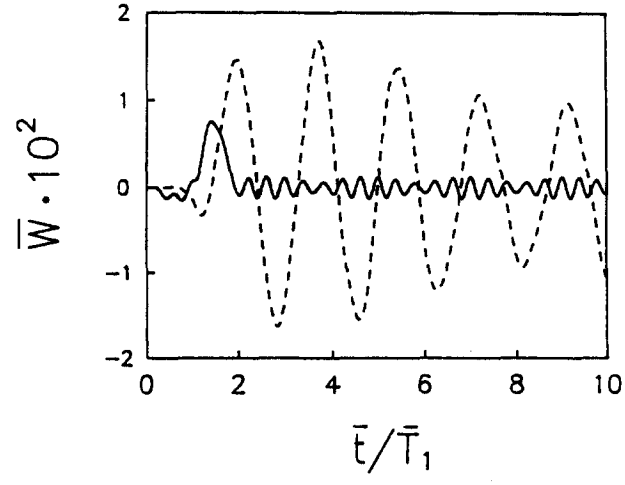

— a=3.19, ····· a=14.37.

Fig. 7 Comparison of two α effects on the history of the middle-point deflection of the second branch of a T-type frame with r_b=0.03 and l_r=0.5 due to a concentrated load.

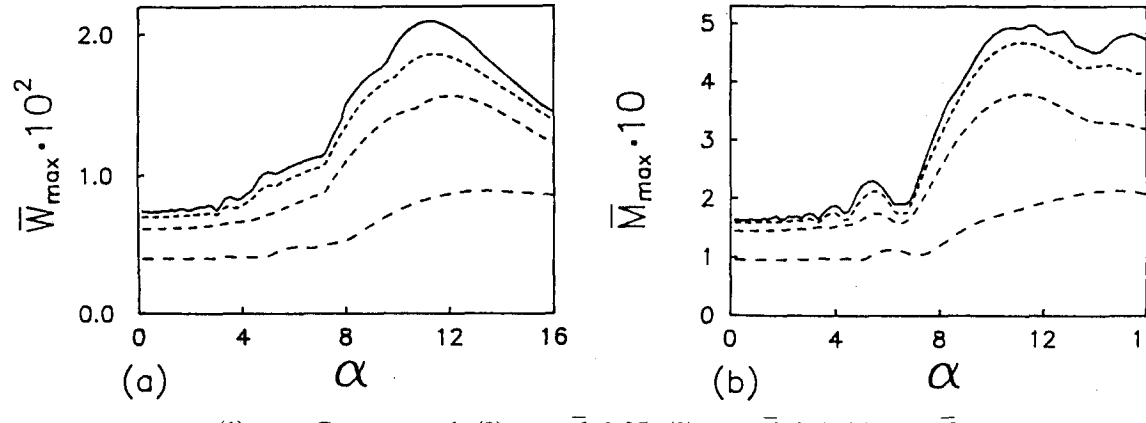

(1) —: Concentrated, (2) —: $\bar{d}$=0.25, (3) ——: $\bar{d}$=0.5, (4) ·····: $\bar{d}$=1

Fig. 8 Comparison of distributed loads on the (a) $\overline{W}_{max}$-α and (b) $\overline{M}_{max}$-α distributions of the T-type frame with r_b=0.03 and l_r=0.5.

r_b=0.03. According to those results, the shorter column length results in higher frequencies. The shorter the column the higher the first modal frequency means that a shorter column induce a more stiffness of the frame. Within the low velocity range $0 \leq \alpha \leq 4$ the load can be regarded as a quasi-static load. Consequently, the shorter column implies that the less value of $\overline{W}_{max}$ is within the velocity range. However, those three l_r effects on the differences of $\overline{M}_{max}$ are not obvious within the velocity range. The first modal frequency of the structure dominates the frame's vibration. The first mode shape is a bending mode. Therefore, the bending wave is the dominant factor on the vibration of the frame. Consequently, both values of α_W and α_M are determined by

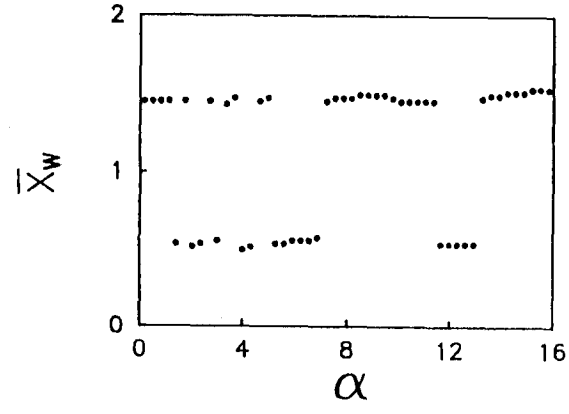

Fig. 9 The $\overline{X}_W$-α distribution of the T-type frame with r_b=0.03 and l_r=0.5 due to a concentrated load.

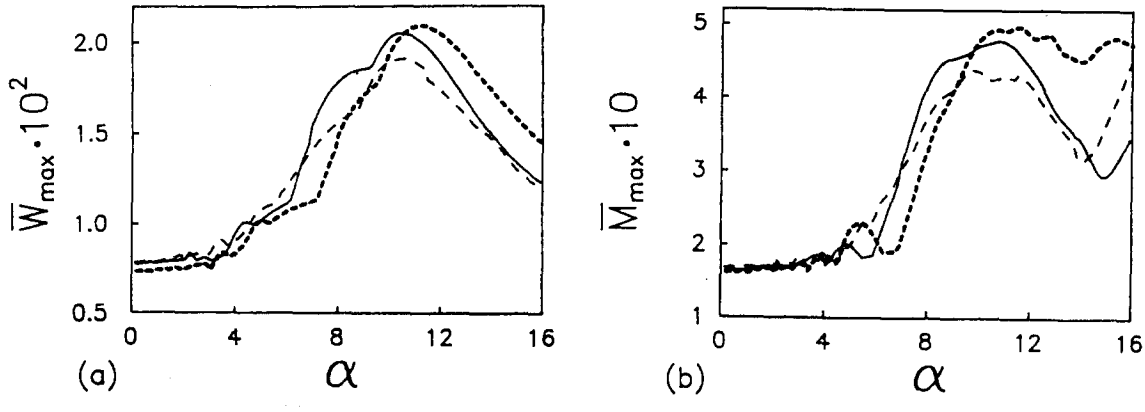

(1) —: I_r=1, (2) ----: I_r=0.5, (3) ·····: I_r=1.2

Fig. 10 Comparison of three l_r values on the (a) $\overline{W}_{max}$-α and (b) $\overline{M}_{max}$-α distributions of the T-type frame with r_b=0.03 due to a concentrated load.

Table 1 Comparison of l_r effects on the fundamental three modal frequencies $\bar{\omega}(=100\ \omega L(\rho/E)^{1/2})$ of a T-type frame with r_b=0.03

	l_r=0.5	l_r=1.0	l_r=1.2
$\bar{\omega}_1$	50.17	43.85	36.13
$\bar{\omega}_2$	59.43	56.88	52.55
$\bar{\omega}_3$	133.76	60.79	55.68

the bending wave. The higher the first modal frequency implies the higher velocity the bending wave. Therefore, both Figs. 10(a) and 10(b) reveal that the shorter the column produces (a) both higher values of α_W and α_M and (b) the greater absolute values of both $\overline{W}_{max}$ and $\overline{M}_{max}$.

8. Conclusions

For a constant-velocity load moving on a T-type Timoshenko frame, there exist a critical velocity at which the displacement of the structure frame becomes absolute large. The maximum deflection at a point of the frame occurs as a load moves at a subcritical velocity on the frame. However, the maximum deflection at the same point will occur after the load left the frame at a supercritical velocity. The critical velocity is larger for the shorter column. The maximum moment always occurs at fixed ends. The maximum deflection always occurs near the middle of one span of horizontal branches.

Acknowledgements

This work was sponsored by the National Science, R.O.C.,. under contract No. 85-2212-E006-112. The financial support is greatly acknowledged.

References

Cheng, F.Y. (1970), "Vibrations of Timoshenko beams and frameworks", *Journal of the Structural Division, American Society of Civil Engineers*, **96**(3), 551-571.

Clough, R.W. (1955), "On the importance of higher modes of vibration in the earthquake response of a tall building", *Bulletin of the Seismological Society of America*, **45**, 289-301.

Herrmann, G. (1955), "Forced motions of Timoshenko beams", *Journal of Applied Mechanics*, **22**, 53-56.

Huang, T.C. (1961), "The effect of rotatory inertial and of shear deformation on the frequency and normal mode equations of uniform beam with simple end conditions", *Journal of Applied Mechanics*, **28**(4), 578-584.

Kolsky, H. (1963), *Stress Waves in Solids*, Dover Publications, New York.

Levien, K.W. and Hartz, B.J. (1963), "Dynamic flexibility matrix analysis of frames", *Journal of the Structural Division, American Society of Civil Engineers*, **89**(4), 515-536.

Rubinstein, M.F. and Hurty, W.C. (1961), "Effect of joint rotation on dynamics of structures", *Journal of the Engineering Mechanics Division, American Society of Civil Engineers*, **87**(6), 135-157.

Shen, J.Y., Abu-Saba, E.G., McGinley, W.M., Sharpe Jr., L. and Taylor Jr., L.W. (1994), "Continuos dynamic model for tapered beam-like structures", *Journal of Aerospace Engineering*, **47**(4), 435-445.

Timoshenko, S.P. (1921), "On the correction for shear of the differential equation for transverse vibrations of prismatic bars", *Philosophical Magazine*, **41**, 744-746.

Warburton, G.B. and Henshell, R.D. (1969), "Transmission of vibration in beam systems", *International Journal for Numerical Methods in Engineering*, **1**, 47-66.

Warburton, G.B. (1976), *The Dynamical Behavior of Structures*, second edition, Pergamon Press, Oxford, England.

Wang, R.T. and Jeng, J.L. (1996), "Dynamic analysis of a T-type Timoshenko frame to a moving load using finite element method", *Journal of the Chinese Institute of Engineers*, **19**(3), 409-416.

Wang, T.M. and Kinsman, T.A. (1971), "Vibrations of frame structures according to the Timoshenko theory", *Journal of Sound and Vibration*, **14**(2), 215-227.